ANNUAL REPORT

AD A126684

COMBUSTION OF AMMONIUM PERCHLORATE-POLYMER SANDWICHES

By

E. W. Price, R. R. Panyam,
J. K. Sambamurthi and R. K. Sigman

Prepared for

OFFICE OF NAVAL RESEARCH
ARLINGTON, VIRGINIA 22217

Under

Contract N00014-79-C-0764

February 1983

GEORGIA INSTITUTE OF TECHNOLOGY
A UNIT OF THE UNIVERSITY SYSTEM OF GEORGIA
SCHOOL OF AEROSPACE ENGINEERING
ATLANTA, GEORGIA 30332

Unclassified

SECURITY CLASSIFICATION OF THIS PAGE *(When Data Entered)*

REPORT DOCUMENTATION PAGE		READ INSTRUCTIONS BEFORE COMPLETING FORM
1. REPORT NUMBER	2. GOVT ACCESSION NO.	3. RECIPIENT'S CATALOG NUMBER
4. TITLE *(and Subtitle)* Combustion of Ammonium Perchlorate-Polymer Sandwiches		5. TYPE OF REPORT & PERIOD COVERED Annual Report Aug. 1981 - July 1982 6. PERFORMING ORG. REPORT NUMBER
7. AUTHOR(s) Edward W. Price, Ramaprasad R. Panyam, Jayaraman K. Sambamurthi and Robert K. Sigman		8. CONTRACT OR GRANT NUMBER(s) ONR Contract No. N00014-79-C-0764
9. PERFORMING ORGANIZATION NAME AND ADDRESS School of Aerospace Engineering Georgia Institute of Technology Atlanta, Georgia 30332		10. PROGRAM ELEMENT, PROJECT, TASK AREA & WORK UNIT NUMBERS
11. CONTROLLING OFFICE NAME AND ADDRESS Mechanics Division, Office of Naval Research Department of the Navy Arlington, Virginia 22212		12. REPORT DATE February 1983 13. NUMBER OF PAGES 40
14. MONITORING AGENCY NAME & ADDRESS*(if different from Controlling Office)*		15. SECURITY CLASS. *(of this report)* Unclassified 15a. DECLASSIFICATION/DOWNGRADING SCHEDULE

16. DISTRIBUTION STATEMENT *(of this Report)*

Approved for public release; distribution unlimited

17. DISTRIBUTION STATEMENT *(of the abstract entered in Block 20, if different from Report)*

Approved for public release; distribution unlimited

18. SUPPLEMENTARY NOTES

19. KEY WORDS *(Continue on reverse side if necessary and identify by block number)*

Combustion, Solid Propellants, Rockets,
Ammonium Perchlorate, Flames

20. ABSTRACT *(Continue on reverse side if necessary and identify by block number)*

A series of experimental studies of combustion of sandwiches is reported, and the results are used to develop a relatively detailed qualitative model for the combustion zone microstructure.

DD FORM 1 JAN 73 1473 EDITION OF 1 NOV 65 IS OBSOLETE

Unclassified

SECURITY CLASSIFICATION OF THIS PAGE *(When Data Entered)*

Acknowledgements

This research has been sponsored by the Mechanics Division of the Office of Naval Research, Arlington, Virginia, under the Contract No. N00014-79-C-0764. The authors wish to convey their appreciation for the patient and thoughtful monitorship of Dr. R. S. Miller, and for the continuity of support so essential to progress in this multifaceted problem.

Table of Contents

Introduction

The combustion of composite solid rocket propellants takes place in a thin region close to the surface of the propellant. The thickness of this region is dictated by the necessity to transfer heat back to the solid at a rate sufficient to maintain the desired rate of pyrolysis at the surface. This in turn dictates that the scale of heterogeniety (usually set by oxidizer particle size) be small enough for fuel and oxidizer vapors to mix in the thin region near the surface. In practice, the dimensional scale turns out to be of order 100 μm, a scale encompassing an entire flame complex. Experimental observation on such a dimensional scale is virtually impossible, a circumstance that has led to a rather speculative quality of research and literature on combustion mechanisms. The situation is further complicated by the uncertain relevance of flame theory when applied to such small, geometrically and chemically complicated flame complexes.

A strategy to alleviate the experimental difficulties of observation is to study combustion of geometrically simple systems such as the oxidizer-binder sandwich. By edge burning such a laminate structure, the combustion zone is constrained to a two-dimensional steady state configuration, hopefully amenable to more meaningful observation and theoretical interpretation. If this goal is achieved, then at least some aspects of the propellant problem can be clarified. Unfortunately, the micro-combustion zone is still substantially inaccessible to experimental observation, even in the geometrically simple systems, so the strategies for research are still less direct than would be desired, and results correspondingly more speculative. One exception to the limitations of spatial resolution in measurements is the quench-burning experiments, which permit leisurely study of the surface of a sample under high magnification. Such

experiments typically interrupt burning very abruptly by rapid depressurization of the combustor. While some artifacts are produced by the quench event, the details of the burning surface microstructure are largely preserved and can be used in combination with other information to infer combustion zone structure.

The quenched sandwich approach has been used by many investigators (e.g., Powling,[1] Hightower and Price,[2,3] Boggs, et al.,[4] Netzer, et al.,[5,6] Nadaud,[7] Ermolaev, et al..[8] It has become evident in recent work[9,10] that relevance to propellant combustion requires that binder laminae in sandwiches be very thin (to avoid anomalous effects such as binder melt flow); and that interpretation of results address observations near enough to the oxidizer-binder interfaces to correspond to situations possible on propellant surfaces. In hindsight, these considerations may seem obvious, but a significant amount of published work on sandwiches of propellant ingredients has addressed situations that were only marginally relevant to conventional propellants. The present studies, involving sandwiches of ammonium perchlorate and typical hydrocarbon binders, used primarily the quench burning method, on sandwiches with binder laminae of 10 - 100 μm thickness. Earlier tests[4,9,10] had shown certain critical features of quenched thin binder sandwiches of interest here, as follows:

1. The larger features of surface profiles are shown in Fig. 1 (See Ref. 9-11).

2. The details in the vicinity of the binder lamina are shown in Fig. 2. Part a shows the trend with binder thickness. Part b shows the trend with pressure (for a binder thickness of 50 - 70 μm). Part c shows certain features of surface quality that are persistent in varying degree for all tested conditions on AP-hydrocarbon binder sandwiches with thin binder laminae, described further below (See Ref. 2-6, 9-16).

3. All test samples from tests above 2 MPa exhibit regions of the AP

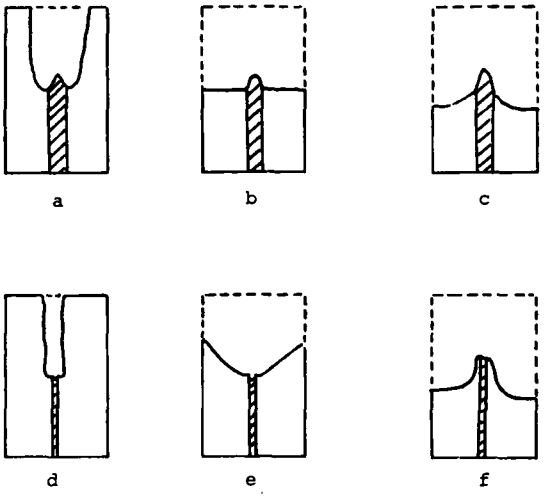

Fig. 1 Cross-section profiles of sandwich burning surfaces (sketched from quenched samples): a) Low pressure (~ 2 MPa); b) Intermediate pressure (~ 5 MPa); c) High pressure (~ 8 MPa); d, e, f) Same as a, b and c, but thin binder (~70 μm).

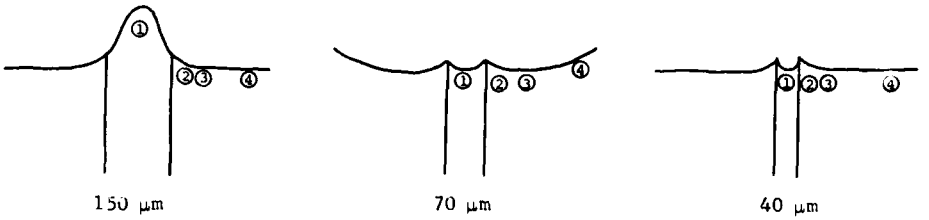

Fig. 2a Profile details, 5MPa, different binder thicknesses:

1. Designates binder surface, protrudes with thick binder laminae (all pressures).
2. Designates AP adjoining binder, protrudes relative to rest of AP surface, relative to binder with thin binder laminae. Surface is smooth, shows binder melt flow with thick binder.
3. Designates outer edge of smooth band, leading edge of AP profile when outer profile is not flat.
4. Designates AP surface typical of AP self-deflagration (surface pattern, flaky residue of reacting froth).

surface ("distant" from the binder lamina) with the characteristic surface qualities of AP self-deflagration, including flaky residue of a surface melt layer, and larger scale surface patterns of ridges and depressions (e.g., Ref. 9-16).

4. All thin-binder test samples showed (Fig. 2a,b) the binder lamina to be recessed relative to the region of the oxidizer laminae immediately adjoining the binder[2-4,9-11] (binder lamina thickness less than 70 μm).

5. All test samples showed a region of the AP lamina centered 25 - 100 μm out from the binder interface plane that was leading the edge of the AP surface regression, i.e., the AP closer to the binder protruded[9-11] (Fig. 2).

6. The surface of the AP in the protruding region showed a distinctive, relatively smooth quality, with no flake relic of the AP melt (Fig. 2c). This smooth band adjoining the oxidizer-binder interface was evident even with a binder (polysulfide) that pyrolized without evidence of a melt state,[9-11] suggesting that the smooth surface was not due to the melt flows commonly observed in thick-binder sandwiches.[2-5,15,16]

Experimental Work

The present experimental work consisted of quenched-burning experiments on sandwiches of PBAN and HTPB binder laminae between AP laminae, and experiments with other materials substituted for the binder to clarify the mechanisms of binder effects. The samples were edge burned at various pressures. Some tests used binder laminae of uniform thickness and were quenched by depressurization at about 500 MPa/sec. Other tests used samples with "tapered" binder thickness ranging from 150 μm at the ignition edge to 10 μm at the opposite edge. The tapered sandwiches were burned at constant pressure below 2.0 MPa. They quenched spontaneously at a binder thickness characteristic of the test pressure. The preparation of samples was described in

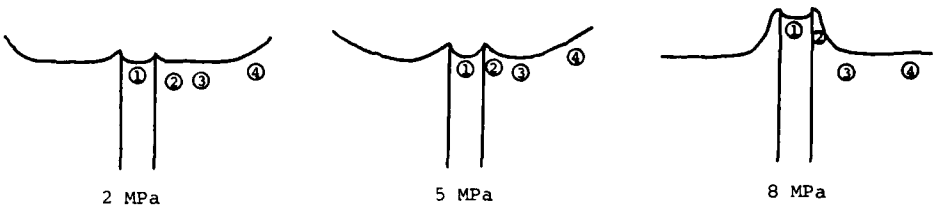

Fig. 2b Profile details, 70 μm thick binder, different pressures:

1. Designates binder surface, recessed relative to adjoining AP.
2. Designates AP adjoining binder, protruding relative to binder and adjoining AP, surface relatively smooth.
3. Designates leading edge of the AP burning front, outer boundary of the smooth band. At high pressures this is the inner edge of a flat AP surface.
4. Designates AP surface, typical of AP self-deflagration (surface pattern, flaky residue of reacting froth). Below 2 MPa, this area has a dry, porous appearance. Above 2 MPa, the slope of this surface indicates sandwich burning rate relative to AP rate.

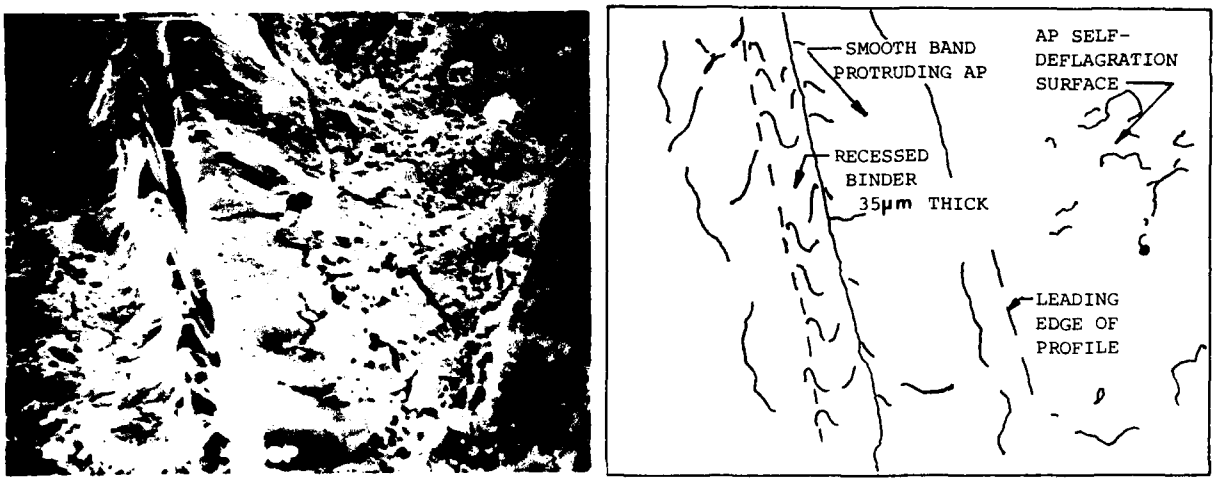

Fig. 2c Details of quenched surface (PBAN binder, thickness 30 μm, pressure 4.14 MPa).

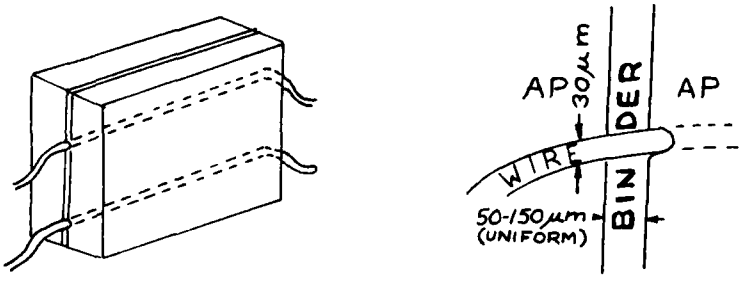

Fig. 3 Wired sandwiches for burning rate measurements.

previous reports[9-11,14] and will not be repeated except for situations not previously reported.

In general, the objective of tests was to measure anything that might reveal something about combustion zone microstructure and controlling processes. This included measurement of burning rate, deflagration limit, structural details of quenched surfaces, and dependence on pressure, binder lamina thickness, and modification of the nature of the binder lamina. Details of procedures and experiments not covered in earlier reports are provided below.

Oxidizer Laminae

These laminae were made by dry-pressing AP powder in a wafer die at 210 MPa for a minimum of 20 minutes.[9,14] Wafer thickness was nominally 1.3 mm. Such pressing cannot produce a totally homogeneous wafer; the particles at the surface are forced to conform to the planar surface of the die, while those in the interior are forced against each other. Because of the importance placed on behavior of the sandwich burning surface in the region of the wafer surface, possible effects of this feature of pressing were examined by two modifications. Sandwiches were tested using AP laminae pressed at lower pressures (131, 61 MPa). Also, AP laminae pressed from finer AP powder (90 μm compared to 110 μm) were tested. The character of the burning surfaces from these various quench tests were not visibly different, indicating that details of the polycrystaline microstructure of the AP laminae had little effect on sandwich burning (examined up to test pressures of 7 MPa). This is consistent with previous observations of similarity between results with pressed AP sandwiches and sandwiches made from AP laminae cut from single AP crystals.[15,17]

Preparation of Sandwiches with Substituted Materials In Place of the Fuel Lamina

Preparation of conventional and tapered sandwiches is described in Ref. 9-11,14. In the present work, some tests were run on sandwiches with the binder lamina omitted or replaced by mica or gold laminae. Since the binder normally serves as a bonding agent as well as a fuel, its elimination poses problems with mechanical integrity of the sandwich and thermal contact between layers. Samples were assembled by holding the laminae together with a metal clip. Perfect thermal contact could not be assured because pressed AP laminae are not perfectly flat, and dry surfaces may be a few microns apart over some of their intended contact surfaces. The wide separation of laminae evident in some of the figures (see Results) is due to removal of the metal clip, necessitated for introduction of the sample into the scanning electron microscope.

AP-Filled Binder Laminae

Addition of fine AP powder to the binder lamina provided a means of modifying the spatial distribution of reactants and the stoichiometry of the binder, and also provided a vehicle for study of the combustion of fine oxidizer particles in a controlled propellant-like environment. Sandwiches were made using 10 μm AP in the binder, in mass ratios of 1:1 and 7:3 AP to binder, using both PBAN and HTPB binder. A nominal lamina thickness of 85 μm was used, with limited investigation of other thicknesses with PBAN binder. After mixing of the AP powder in the uncured binder, preparation of sandwiches was similar to that without AP. Lamina thicknesses less than 45 μm were very difficult to make because of viscosity of the binder-AP mix and presence of some clumps of AP larger than the nominal 10 μm size. Table 1 summarizes the test conditions used.

Table 1

Test conditions for sandwich tests with AP-filled binder laminae
10μm AP, lamina thickness approximately 80μm, unless noted otherwise

Serial No.	Variable \ Pressure	1.4 MPa (200 psi)	4.2 MPa (600 psi)	6.9 MPa (1000 psi)
1	Control - PBAN binder	X	X	X
2	1/1 AP/PBAN	X	X	X
3	7/3 AP/PBAN	X	X	X
4	Control - PBAN Binder	X	X	X
5	1/1 AP/HTPB	X	X	X
6	7/3 AP/PBAN lamina 40μm thick			X
7	7/3 AP/PBAN lamina 140μm thick			X

Measurement of Binder Lamina Thickness

Control and measurement of thickness of thin-binder laminae is very difficult. Nominal thicknesses were assigned on the basis of thickness of spacer shims used in fabrication of samples. In burning rate tests, one edge of the sample was viewed in the scanning electron microscope, and average thickness was determined from measurements at five points. In spontaneous quench tests of tapered samples, the thickness at quench was determined by SEM examination (a minimum of five points were measured on the burned surface). Similar measurements were available from SEMs of flat binder samples from rapid depressurization quench tests, but only average values are reported.

Surface Profiles

The profile of the burning surface is referred to throughout the report. Efforts were made to section samples, or replicas of samples, to get direct views of profiles for measurement. However, the pressed AP laminae are too fragile and structurally disorganized to cut. Preliminary efforts to obtain cut sections of plastic replicas showed promise, but were not completed due to lack of time. Currently, work is in progress on profile measurements of quenched surfaces using an optical microscope with a shallow depth of field lens and calibrated lens and sample positioning controls. Quantitative determination of profiles was limited to measurements of lamina thicknesses, and slope of the quenched AP surfaces of "V"-shaped profiles (for use in burning rate calculations; see below). Other details of profiles in the report are described in qualitative or comparative terms, based on observation of the samples in optical and electron microscopes (SEM).

Burning Rate

It is not particularly easy to measure burning rate of thin-binder sandwiches. An effort was made to do so using break wires in the sandwich (Fig. 3). The original objective was to determine the effect of binder lamina thickness on burning rate, in the 30 to 300 μm thickness range. The wires were 30 μm diameter copper, set in scribed grooves in the AP lamina and bonded in place by the binder lamina material and its curing process. The wires were connected into a suitable D.C. source and current measuring circuit that indicated the change upon burnout of each wire. Results were not as reproducible as would be desired; they are summarized under Results.

A second strategy for estimating burning rate involves observation of the angle of the "V"-shaped profile that results when the interface region burns faster than the AP further out from the fuel lamina (Fig. 1 e). This method[16] is applicable at intermediate pressures, above the AP self-deflagration limit. Using the known burning rate of AP, and assuming that the AP far from the fuel lamina burns at that rate, the angle θ of the "V" indicates the rate of regression of the sandwich profile

$$r_s = r_{AP}/\sin(\theta/2)$$

The angle θ is measured from quenched samples that have burned long enough to establish steady state profiles. In the present report, only qualitative (comparative) determinations of burning rate were made by this method.

Results

Surface Profiles and Burning Surface

The present work has involved a variety of tests designed to identify and clarify the dominant processes during sandwich burning. In most cases, the present tests were motivated by some preconception of controlling processes, which will be noted later and compared with the outcome of the test. In all tests except those noted specifically in the next paragraph, the results consistently confirmed the generalizations 1 - 6 noted in the Introduction and based on earlier work on thin-binder sandwiches.[9-11,14]

One specific combination of tests is most directly applicable to the issue of surface profiles and microstructure. In this combination of tests, the binder lamina was replaced by mica, by gold, and by simple omission of the binder lamina. Typical results of tests at 4.2 MPa are shown in Fig. 4. Part a is from a control test with a 100 μm thick lamina of PBAN. Part b shows the details of the sandwich surface from a 4.2 MPa test on a sandwich with a mica lamina in place of the binder. The detail shown is typical of the interface region in these tests. It is also typical of the self-deflagration of AP, normally exhibited on AP laminae of sandwiches at surface sites further from the interface. With mica laminae there was no smooth band and no protrusion of AP in the interface region. Part c shows the quenched surface of a sample consisting simply of two AP laminae held together during burning by a metal clip. The figure shows the characteristics of simple AP deflagration, uninterrupted up to the interface plane. Under high magnification it is evident that the surfaces of the two slabs were together during burning; surface patterns near adjoining edges are

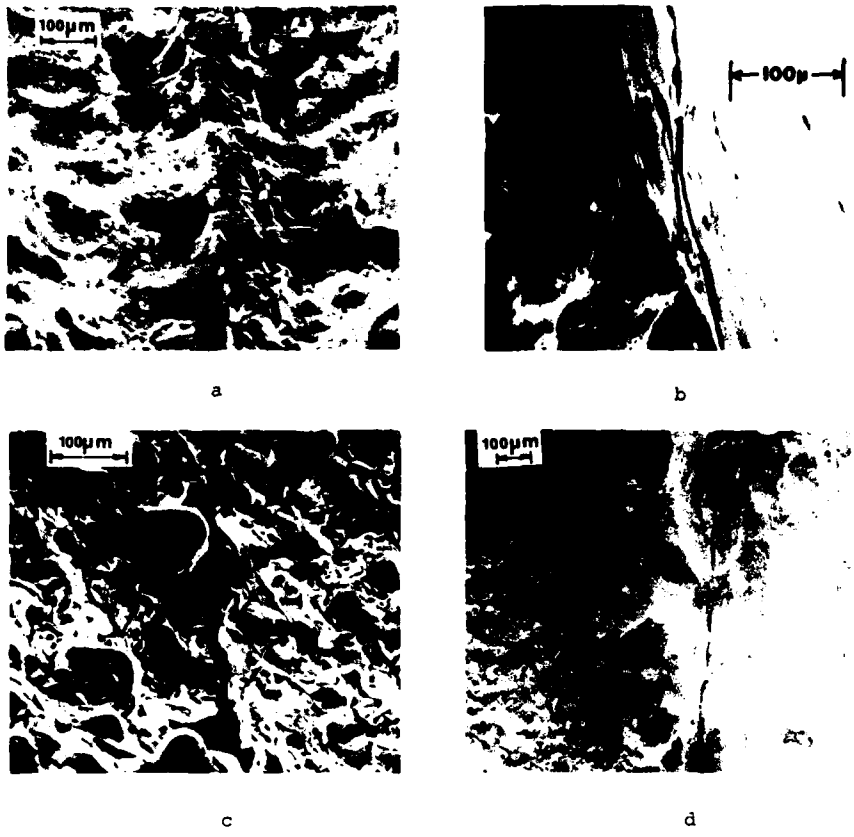

Fig. 4 Sandwiches with substitutions for binder lamina (pressure 4.2 MPa)
a) PBAN binder, approximately 100 µm
b) Mica lamina
c) No lamina (2 AP slabs, initially in contact)
d) Gold lamina

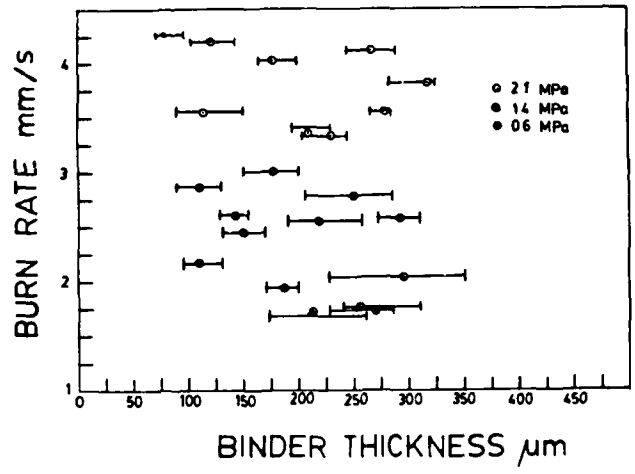

Fig. 5 Sandwich burning rate vs binder thickness, PBAN binder.

correlated, and the edges show matched features indicative of separation of a contiguous liquid surface layer. There is no protrusion of the AP laminae in the interface region. Part d shows the quenched surface of an AP sandwich in which the binder lamina was replaced by a 15 μm layer of gold. Such samples consistently showed retarded burning (protruding AP) in the vicinity of the gold lamina, and a relatively smooth surface there. This behavior was not as uniform along the lamina as with a binder lamina, but was predominant. The nonuniformity may be due to the difficulty in achieving uniform thermal contact between laminae. It is stressed here that the "smooth band" phenomenon described here is not a manifestation of the binder melt flow reported in many earlier studies. With thin-binder sandwiches, melt flow is minimal,[4,9] and the smooth band is present even with a non-melting polysulfide binder[9] and with the gold lamina.

Burning Rate

The break-wire method was used to conduct a series of tests to relate sandwich burning rate to pressure and binder lamina thickness (PBAN binder). The experimental results are summarized in Fig. 5 and 6. The scatter of data is too large to reveal any trend of burning rate with binder lamina thickness (the original objective of the tests; see Ref. 10,11). Experimental difficulties limited the yield of test work on samples with binder thickness below 100 μm, the most serious problem being nonuniformity of binder lamina thickness. Figure 6 shows the dependence of burning rate (average of all lamina thickness) on pressure. The broken line curve is the AP deflagration rate, from Ref. 17. The binder lamina does not appear to increase sandwich burning rates above about 4.2 MPa.

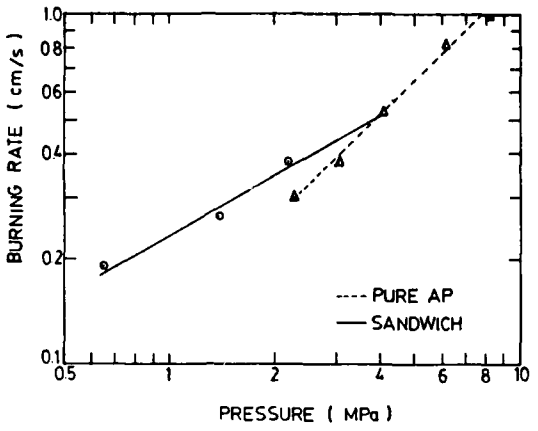

Fig. 6 Sandwich burning rate and AP burning rate vs pressure. PBAN binder, thickness 100 - 300 μm.

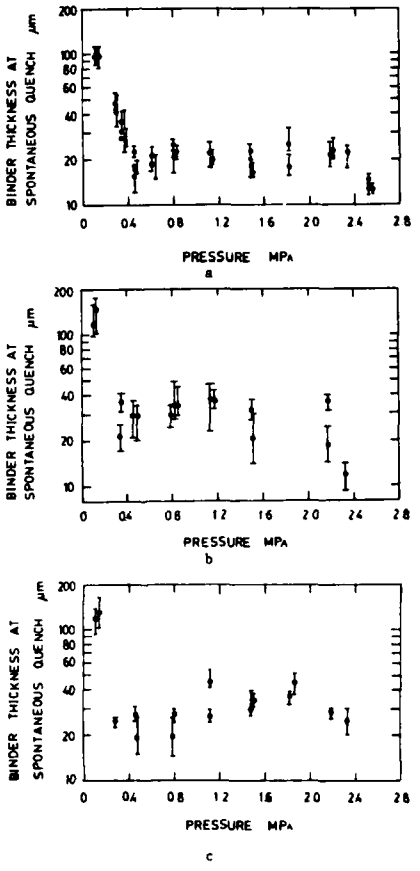

Fig. 7 Deflagration limits for tapered binder sandwiches burned at constant pressure and spontaneously quenching at the indicated binder thickness:
a) PBAN binder; b) PS binder; c) HTPB binder.

In the present studies it has been observed[9-11,14] that in this higher pressure range, quenched sandwiches such as those represented in Fig. 5 and 6 (PBAN binder laminae of thickness > 100 μm) exhibit flat surface profiles, protruding in the immediate vicinity of the binder when tested at pressures in the 4.2 - 7.0 MPa range (Fig. 1b,c). Sandwiches with thinner binder showed "V"-shaped profiles (Fig. 1 e).

Low Pressure Deflagration Limit

Results of the spontaneous quench tests on tapered sandwiches are summarized in Fig. 7 for three binder materials. Over the range of 0.4 - 2.0 MPa, the sandwiches with any particular binder tended to quench at nearly the same binder thickness. Above 2.0 MPa, samples usually burned to completion, a result that is consistent with the fact that AP self-deflagrates above 2.0 MPa. At pressures below 0.4 MPa, the binder thickness for self quenching became increasingly pressure dependent. Limited testing was made with samples with different degrees of taper of the binder lamina to test the possibility that the quench limit might be dependent on details of the approach to the limit. No statistically significant effect was evident. The different binders yielded significantly different quench limits in the 0.4 - 2.0 MPa range. Figure 8 shows a scanning electron microscope picture of a spontaneously quenched sample. The general features are similar to those of samples with binder lamina of uniform thickness quenched by rapid depressurization from comparable pressures. The thickness measurements in Fig. 7 were obtained from similar SEM pictures of suitable magnification.

Fig. 8 Scanning electron microscope picture of the surface of a sandwich from a deflagration limit test.

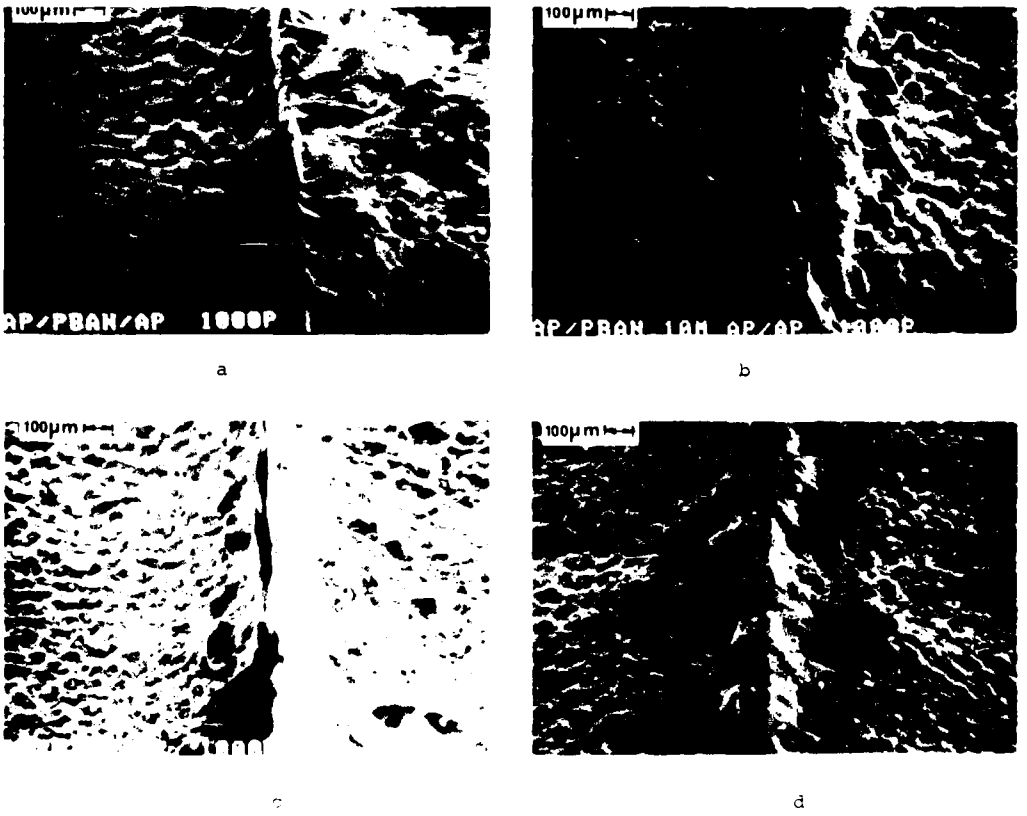

Fig. 9 Surfaces of samples with (a,b) PBAN binder and (c,d) HTPB binder, (a,c) without AP in the binder and (b,d) with AP in the binder. Quenched from 6.9 MPa.

AP-Filled Binder Laminae Sandwiches

Results of tests are summarized in Fig. 9 - 11. Figure 9 shows a comparison of quenched sandwiches with pure binder and with 1:1 AP-filled binder. From these tests (6.9 MPa) there is an obvious difference between behavior of sandwiches with and without AP in the binder. From extensive examination of samples with 1:1 laminae, it is evident that the region of protruding AP is widened and protrudes less. The protruding region is flat on top, and the surface quality is smooth. The binder lamina is recessed and the surface of that lamina shows undulations of the same dimensional scale as the AP filler. However, no distinguishable AP particle surface is evident there. The details conform qualitatively to the general features 1 - 6 noted in the Introduction, but differ unambiguously from those of sandwiches with pure binder laminae in the details noted above. The differences become less evident at lower pressures. The difference between the results with the two binders is evident in Fig. 9 and similar with either filled or unfilled laminae.

Use of a higher mass ratio of AP to binder in the "binder" lamina (7:3) produced more conspicuous results. At 6.9 MPa, the filled lamina caused an overall sandwich burning rate that was higher than the AP rate, leading to a "V"-shaped surface profile (Fig. 10). The extent of this effect was dependent on the thickness of the lamina. The details of the profile in the vicinity of the interface plane were examined in the SEM and found to be still in agreement with the six general characteristics listed in the Introduction. Specifically (Fig. 9, 10), there was a slight retardation of the AP regression (protrusion) immediately adjacent

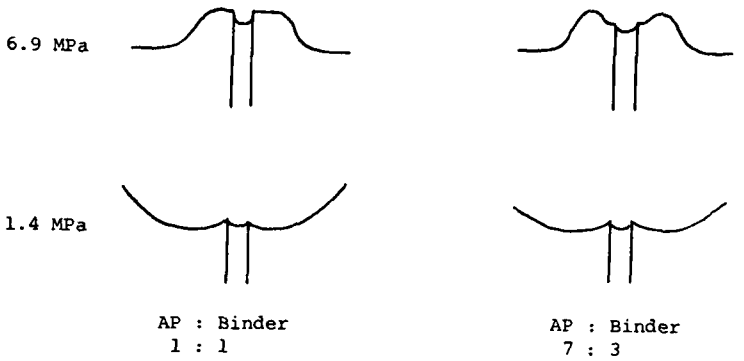

Fig. 10 Surface profiles of sandwiches with different AP:binder ratios in the binder laminae and different pressures. PBAN binder.

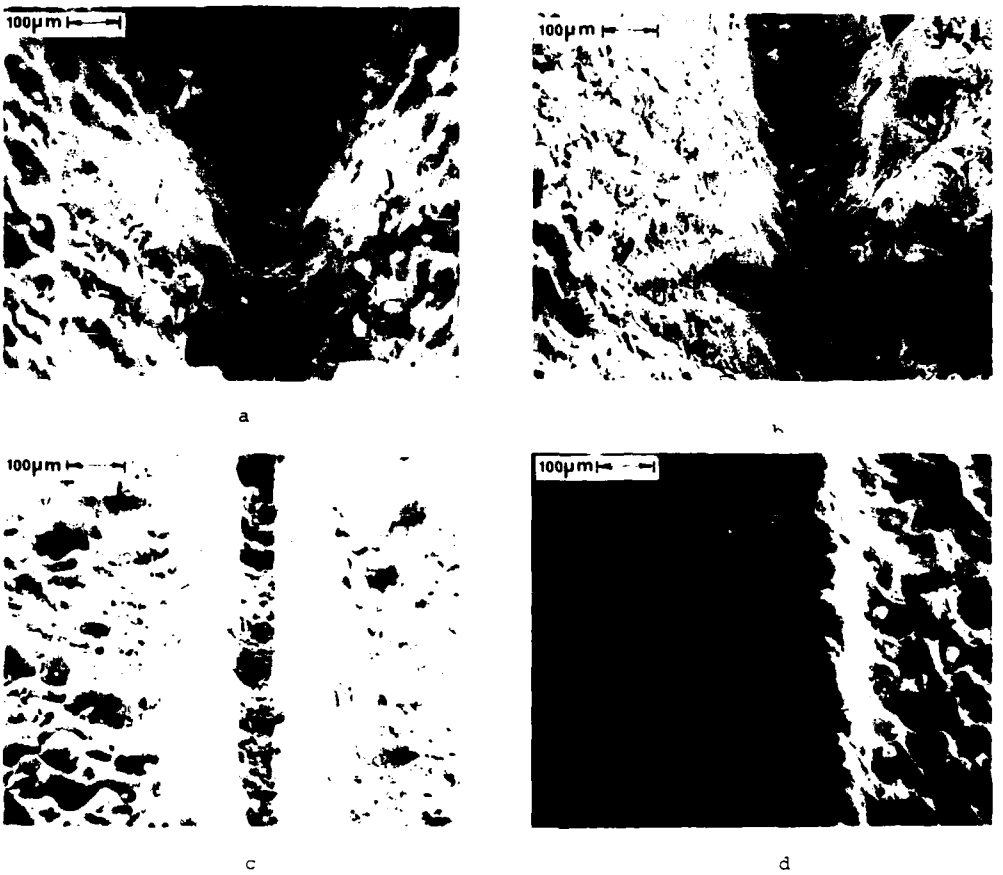

Fig. 11 Effect of lamina thickness on quenched surface with AP-filled PBAN binder laminae (SEMs). AP:binder ratio 7:3, 6.9 MPa.

to the lamina interface plane, with a small smooth band. The binder was recessed, and the leading edge of the AP front was at the outer edge of the smooth band. The retarded AP and smooth band were less conspicuous than with pure binder laminae. The most conspicuous feature was the dependence of profile on thickness of the filled binder lamina. At 45 μm, the profile was very similar to those with 1:1 AP-binder, while the "V" profile increasingly steepened as lamina thickness was increased (Fig. 11).

Discussion

There are some features of combustion of AP-hydrocarbon binder systems that are generally accepted, at least in qualitative terms. These are noted below as a basis for interpretation of the present results.

1. Ammonium perchlorate self-deflagrates at pressures above about 2 MPa. This pressure is sensitive to ambient temperature, partly because of the rather modest flame temperature.[12,13,18,19]

2. Self-deflagration of AP proceeds by a combination of a complex reaction in a surface liquid or froth, along with a gas phase flame. Heat release occurs in varying degree in both sites.[2-5,12,13,18,20,21]

3. Heat release in reactions between AP and hydrocarbon binders occurs primarily in the gas phase.[2,4,9,16,18] (Contrary views can be found in early literature.)

4. Burning rates of the composite systems are dependent on the structural details of the systems. This is generally attributed to the effect of propellant microstructure on location of gas phase reaction sites (flames) (e.g., Ref. 22).

5. The gas phase flames consist of a leading edge portion involving vapors that have already mixed, and a trailing portion governed by continued diffusion of oxidizer and binder vapors. The leading edge portion is described as having the properties of a kinetically limited pre-mixed flame, and the trailing portion has the properties of a diffusion-limited flame.[11,18,22-25] Details and relative importance of the two portions of the flame are matters of speculation.

Profiles and Substitutions for Binder Laminae

The details of the quenched burned surfaces of sandwiches presumably reflect the consequences of flame and surface reactions and associated heat flow in the gas and solid. In looking at these details, the protrusion of the AP in the vicinity of the oxidizer-binder interface planes seems to require that the surface in that region be at lower temperature than on the immediately adjoining AP surface. The smooth character of the surface suggests that the exothermic reacting froth is absent. One may argue that the lower temperature caused the surface vaporization to shift to a dissociative sublimation process. Alternatively, one may argue that some unknown process intervened in the froth reaction, or that the smooth surface is an artifact of the quench event. The most likely interpretation seemed to be that there was a net lateral heat flow from the exothermic AP lamina to the endothermic fuel lamina, limited to a region of the order of the thermal wave thickness in the solid induced by the combustion wave. Such a heat drain effect, suggested by various authors (e.g., Ref. 26,27), would locally reduce the oxidizer surface temperature and reaction rate, the effect being augmented by a corresponding shift of oxidizer heat release from the surface froth site to the flame site or beyond. The width of the

region of protruding AP and smooth band is of the same order as the thermal wave thickness, consistent with this interpretation. The tests with mica laminae (Fig. 4b) were made to test the postulate that, in the absence of heat flow from the oxidizer lamina to the endothermic lamina, the AP would regress normally, i.e., without retardation or modification of surface processes. Mica was chosen as a binder substitute because of its low thermal conductivity, and availability in thin sheets with flat surfaces. The test unequivocally conformed to the postulate; the AP surface was flat up to the interface plane with the mica, and the surface patterns and relic of froth typical of AP self-deflagration extended all the way to the interface.

The foregoing interpretation left open the possibility that some other (unknown) effect of binder was responsible for "anomalies" in the AP deflagration near the interface (e.g., the binder melt flow effects evident with thick binder sandwiches). To further test the postulate that lateral heat drain from oxidizer to binder was the cause, the heat conducting gold laminae were used. These tests showed that retarded AP regression and smooth bands occurred with a heat-absorbing lamina in complete absence of binder (Fig. 4d) , indicating that lateral heat drain is the primary cause. The local transition of AP surface vaporization to a less exothermic mode probably enhances the retardation of the surface regression. The tests with two AP laminae in direct contact (Fig. 4c) were made to assure that the absence of a "wetted" surface did not play some unanticipated role in the results. As noted earlier, the two laminae of AP, held together in the same manner as the "mica sandwiches" and "gold sandwiches", burned as if they were a single lamina. Collectively, the results make a strong case for the lateral heat drain as the cause of profile and surface details near the interface plane, with shift in surface decomposition of the AP (to dissociative sublimation)

playing a role. Given the consistently recessed state of the binder lamina, this seems to require that the binder surface be cooler than the oxidizer surface. This conclusion is at odds[18] with the limited data available on high temperature binder pyrolysis (e.g., Ref. 28), and is being examined more carefully through heat transfer computations.

The Gas Phase Combustion Zone

While observation of details of the gas phase flame have not been made directly, a reasonable description can be constructed from basic concepts of flames. Consider for example the problem of combustion down a single contact interface between a fuel slab and an oxidizer slab (Fig. 12). The vapors flow away from the surfaces of the slabs, diffusing into each other to form a mixing fan and stoichiometric surface starting at the sample surface, along the interface plane. On the dimensional scale of interest, the diffusion is likely to be molecular, forming a nonuniform (two-dimensional) "pre-mixed" region of oxidizer and fuel vapors. At some point in this mixing region conditions may become favorable for establishment of a pre-mixed flame. Reaction kinetics will presumably dominate the standoff distance of this flame; the stoichiometric surface is the most favorable site for the leading edge of the flame because of higher temperatures possible there. The flame will trail laterally into the nonstoichiometric part of the mixing region in a manner limited by concentration and temperature profiles. On the scale of interest here (of order 10 - 100 μm), it is uncertain whether a stable thin flame sheet is an accurate detailed description, although flames of this type have been observed in stratified

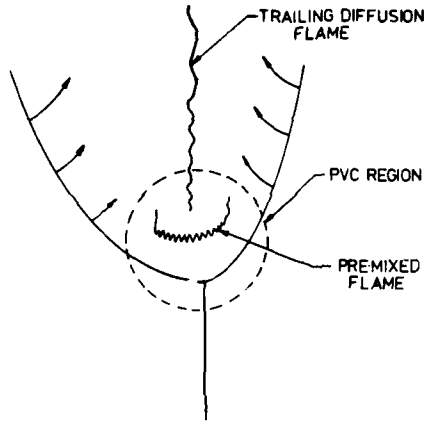

Fig. 12 Model of burning down the interface between an oxidizer and a fuel slab.

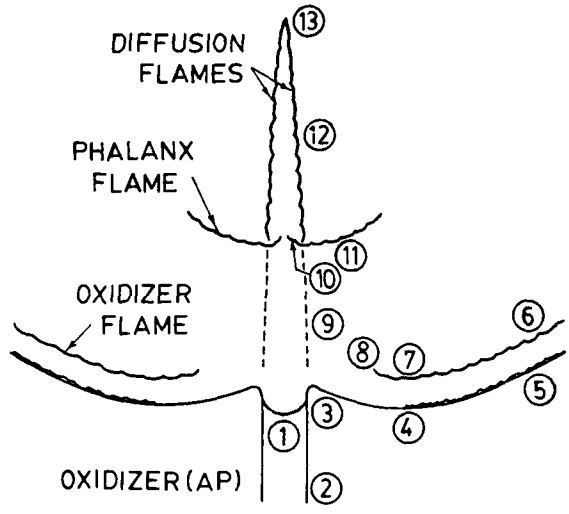

Fig. 13 Principal features of combustion zone microstructure suggested by experimental results.

1. Binder lamina: recessed relative to adjoining oxidizer.
2. Interface plane between oxidizer and binder.
3. Oxidizer, protruding relative to binder and adjoining oxidizer. Surface is characteristically smooth.
4. Oxidizer, leading edge of the oxidizer profile. Surface exhibits frothy character attributed to exothermally decomposing "melt".
5. Oxidizer, region that regresses at normal self-deflagration rate (details depend on relative rate of oxidizer, sandwich). Surface exhibits same characteristics as pure oxidizer deflagration.
6. Oxidizer flame, typical of oxidizer self-deflagration.
7. Oxidizer flame, supported by heat from secondary flame.
8. Oxidizer flame, attenuated or quenched by subsurface heat loss to endothermic binder.
9. Stoichiometric surface in oxidizer-binder diffusion fan.
10. Phalanx flame: fuel-rich branch, extends out to a "flammability" limit.
11. Phalanx flame: oxidizer-rich branch, extends out to a flammability limit.
12. Diffusion-limited reaction zone, height depends on lamina thickness.
13. Closure of stoichiometric surfaces and associated pair of diffusion flames (flame tip).

mixtures of methane and air at atmospheric pressure.[29] Kinetically-limited reaction regions, of somewhat more diffuse nature, are postulated in various models of combustion of heterogeneous systems.[22-25,30,31] The representation as a flame sheet here is primarily for convenience in distinguishing it from other reaction regions. In most situations the kinetically-limited flame is the leading edge for a diffusion-limited flame region, and will be referred to here as the "kinetically-limited leading edge flame," or "KLLEF".

In Fig. 12, the region immediately behind the KLLEF is hot, and reaction proceeds as rapidly as diffusion mixes the flows on either side of the stoichiometric surface. Further out, this diffusion limited region approximates a classical diffusion flame, with oxidizer and binder vapors that have come directly from the surface without going through the KLLEF.

In Fig. 13, the details of surface and AP flame behavior,[2,3,12,13,32] and AP-binder two-slab flame behavior (Fig. 2 and 12) are combined to show the general features of the sandwich combustion zone. Features are noted by the numbers, and explanations in the figure legend. Depending on the thickness of the binder lamina, the sandwich burns as two relatively independent (two-slab) combustion zones, or as interacting combustion zones when binder is thin. From the standpoint of burning rate, there is a leading portion of each two-slab combustion zone (including the KLLEF) that dominates the burning rate,[11,24,31] and more remote portions that supply minimal heat to the leading edge of the burning front. The leading portion has been called the "propagation velocity controlling" (PVC) region,[11,31] and is probably dominant in controlling not only propagation velocity, but other combustion behavior as well (e.g., combustion stability). The interaction of the two combustion zones in a burning sandwich is probably not important unless the binder is thin enough for the PVCs to interact (exact

thickness depending on definition of what is important, and on size of the PVC and its dependence on pressure). This concept of interaction is illustrated in Fig. 14, and will be pursued further later in the context of specific experimental results.

Deflagration Limits

The qualitative model of the combustion zone provides a framework in which to interpret the deflagration limits reported in Fig. 7. Consider first the trend of results at low pressure. With a thin-binder lamina, the interaction of the PVCs is extensive. In particular, the diffusion fans from the two oxidizer-binder interfaces merge, and the two stoichiometric surfaces close in a "tip" (Fig. 13) over the binder relatively near the sample surface. Under these conditions, the KLLEFs may not occur in the mixing fans, especially at low pressure. In a specific deflagration limit test (constant pressure, tapered binder lamina), the flame situation would progress as in Fig. 15, with the stoichiometric tip retracting until it is below the normal KLLEF position for that pressure. The region above the stoichiometric tip is oxidizer rich, and increasingly so with distance from the sample surface. Thus the flame temperature and its trend with distance are unfavorable for a stable KLLEF immediately above the stoichiometric tip. It is postulated that retraction of the stoichiometric tip below the normal KLLEF position leads to quench, and that this is what happens at low pressure when the limiting binder thickness is approached.

Following the above postulate, the pressure dependence of the deflagration limit can be examined by examining the trend of KLLEF standoff and

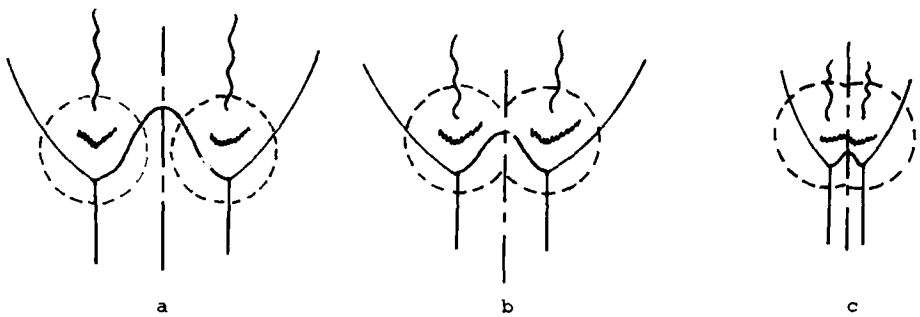

Fig. 14 Effect of reducing fuel lamina thickness (showing onset of PVC region interaction): a) intermediate thickness; b) thin binder; c) very thin binder.

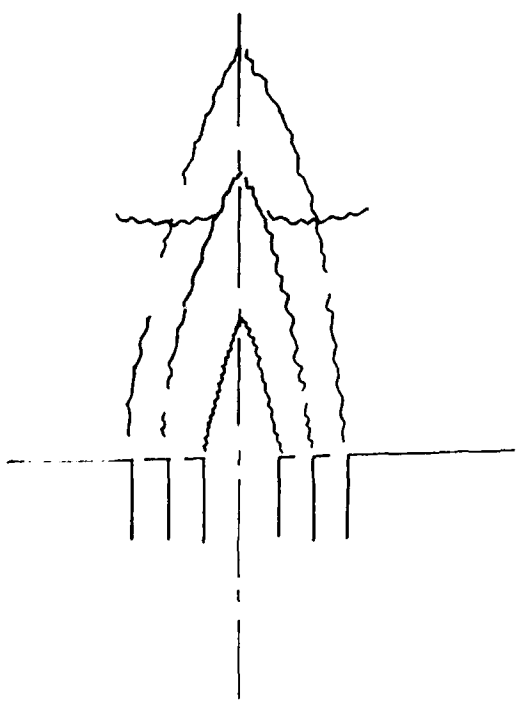

Fig. 15 Stoichiometric tip retraction due to decreasing binder thickness.

and stoichiometric tip height with increasing pressure. Looking first at the pressure dependence of the stoichiometric tip height, an estimate can be made on the basis of classical models of diffusion flame height (e.g., Ref. 33). Such models, which are based on diffusion rates, yield a nondimensional height of the stoichiometric tip,

$$\eta_t \equiv k z_t D/v = k z_t \rho D/\rho v$$

where k depends on the geometrical arrangement, z_t is the actual height, D is a diffusion coefficient, and v is the convective flow velocity. In such analyses it is usually satisfactory to assume that the product ρD is independent of pressure. The pressure dependence of ρv can be estimated from the pressure dependence of the burning rate, usually approximated by the relation

$$m/\rho_p \equiv r = Cp^n = \rho v/\rho_p$$

where ρ_p is the density of the solid. Combining these relations, the pressure dependence of the stoichiometric tip height is

$$z_t \propto \rho v \propto p^n$$

Typical values of n are between 0.2 and 0.5 for AP composite propellants, and the value for the tests in Fig. 6 is roughly 0.55. Thus the height of the stoichiometric tip decreases with decreasing pressure.

The dependence of the standoff distance of the KLLEF on pressure can be estimated from thermal flame theory (e.g., Ref. 34). For the present values of

surface and flame temperatures, an adequate approximation is provided by

$$z_f \propto 1/m = 1/\rho_p r$$

$$z_f \propto p^{-n}$$

This means that the flame standoff distance increases with decreasing pressure, while the stoichiometric tip height is decreasing. Thus it is plausible that there would be a critical lower pressure limit for existence of the KLLEF, and that the pressure-dependent part of the binder thickness limit curves in Fig. 7 reflects such a limiting mechanism. The chemistry and the geometry of the situation preclude quantitative analytical determination of such a limit at present, but the experimental results and the qualitative interpretation help in description of the flame structure. In practice, the pressure dependence of the flame standoff is probably much greater than that indicated by the above argument, because the pressure exponent, n, reflects effects of the diffusion controlled part of the flame as well as the more pressure-dependent kinetically limited part of the flame, while the diffusion flame probably exerts very little influence near the quench limit.

The change in the deflagration limit curves to relatively low pressure dependence above 0.4 MPa indicates emergence of different controlling factors. To examine this, it helps to recall the physical situation prevailing during sandwich burning at low pressure. During the constant pressure burning of a tapered sandwich, the burning front proceeds down a "slot" between two walls of AP (Fig. 1a, 1d). Lateral heat flow into the AP walls is a drain on the heat balance, in the sense that such heat is not returned to the flame or PVC region. As the binder lamina becomes thinner, first the outer flame, and then the flame

in the PVC region shrinks due to limited fuel supply. In effect, the heat supply decreases, and the lateral heat drain becomes disproportionately large. The result is decreasing flame temperature, which must ultimately bring reaction kinetics into dominance and lead to quenching. The experimental results indicate that above 0.4 MPa this approach to quench is dominated by individually or collectively pressure insensitive processes. Extrapolation of the low pressure results (dotted line, Fig. 16) suggests that the stoichiometric tip does not retract below the normal position for the KLLEF in the > 0.4 MPa range; however, the KLLEFs eventually "feel the heat drain", and move out due to cooling as the quench event develops, and the conditions ultimately responsible for quench may include shift of the KLLEFs beyond the stoichiometric tip. Lacking a more rigorous description of the combustion zone, it may not be possible to explain why the trend in the 0.4 - 2.0 MPa range is so nearly pressure independent. The major role of thermal and molecular diffusion (in determining heat balance and the flame downstream of the KLLEFs) no doubt plays a role.

A further feature of the results of deflagration limit measurements was the dependence of the limiting binder thickness on the kind of binder. The possibility that the limit values were dependent on stoichiometric flame temperature was considered, but the limits do not exhibit the inverse dependence on flame temperature one would expect. Other properties of the binder of possible importance are thermal conductivity, heat capacity, pyrolysis kinetics, tendency to form a melt on the surface, diffusion coefficients of pyrolysis products, and chemical kinetics of binder-oxidizer vapor reactions. However, there is not sufficient information on most of these properties to make any convincing interpretation.

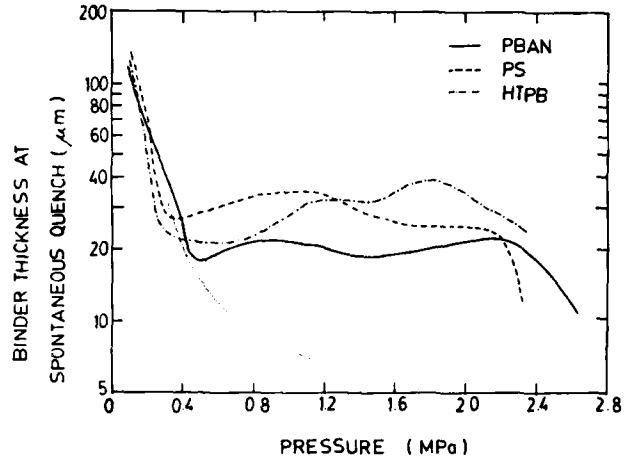

Fig. 16 Deflagration limits, and postulated condition for stoichiometric tip retraction (lower curve).

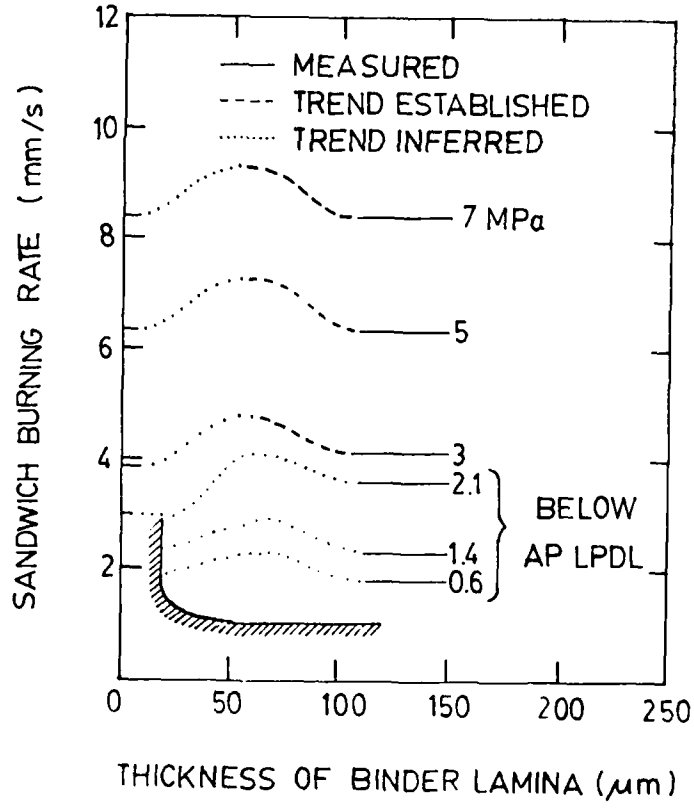

Fig. 17 Dependence of sandwich burning rate on thickness of binder lamina and pressure. Solid portions of the curves are based on quantitative results; broken portions are based on qualitative results; dotted portions are postulated.

Burning Rate and Combustion Zone Microstructure

Burning rates of composite propellants are normally dependent on particle size of ingredients, and one might expect to find conditions under which the burning rates of sandwiches are dependent on lamina thickness.[8,10,11] Assuming the "PVC" region concept is valid, the dimensions of the PVC region could be estimated from experimental determination of the range of binder thickness over which sandwich burning rate is sensitive to thickness. In addition, the specific effects of binder thickness presumably would provide clues to details of the flame structure in the PVC. In the present studies, the experimental results consisted of the direct measurement of burning rate (Fig. 5 and 6), and observations of the angles of the surface of samples with "V"-shaped profiles. As noted in Fig. 5, the direct measurements of burning rate did not show any dependence of rate on thickness in the thickness range 100 - 300 μm. The scatter in data and limitation in thicknesses to the 100 μm-plus range leaves the issue of rate dependence on thickness unresolved. However, a review of conditions for "V" surface profiles (in the 2 - 7 MPa pressure range) indicates that burning rate is higher in the 50 - 100 μm range of binder thickness. This is elaborated below in the context of the general trend of sandwich burning rate vs. pressure.

If one compares (Fig. 6) the measured sandwich burning rate with AP self-deflagration rate reported elsewhere,[13,15,17] it is seen that the AP rate increases more rapidly with pressure than does the sandwich rate, with the two curves crossing at about 4.2 MPa. With such sandwiches (binder lamina 100 - 300 μm thick), the quench profiles are typically flat with protruding binder lamina at pressures above 4.2 MPa (Fig. 3b). However, a reexamination was made of

quench tests on sandwiches with thin binder (50 - 100 μm), and it was found that "V"-shaped profiles were obtained consistently up to as high as 6.9 MPa. This result indicates that the sandwich burning rate with thin-binder sandwiches is higher than either the AP rate or thick-binder sandwich rate in the 3.2 - 6.9 MPa pressure range (AP rate and thick binder sandwich rates are the same in this pressure range, being dominated by the AP rate). There is no obvious reason to expect this trend with binder thickness to disappear at lower pressure, so it seems likely that direct measurement of burning rate done at lower pressure would have revealed an increase in rate with decreasing binder lamina thickness below 100 μm (Fig. 5), if measurements could be made on thin-binder sandwiches.

The struggle to test for increased burning rate at low binder thickness was motivated by a qualitative mechanistic argument that was first stimulated by interpretation of the spontaneous quench limit data. This argument was introduced earlier in the context of Fig. 14. With thick binder laminae, the PVC flames above each interface plane lose heat by lateral conduction to both oxidizer and binder that does not contribute to the PVC flames (i.e., doesn't go through the PVC flame). This heat is lost to the PVC flame, with a corresponding decrease in possible burning rate. As the thickness of the binder lamina is reduced, the heat lost to the binder that flows away between the two PVC flame regions is decreased, simply because the PVC regions begin to merge. A corresponding increase in burning rate would be expected, provided other compensating effects are secondary. It was this increase in burning rate that was sought in the burning rate tests. The binder thickness at which it occurred would be a qualitative indication of the width of the fuel-rich portion of the PVC region of the sandwich flame. The results indicate that this width is of order 70 μm. According to this interpretation, only the PVC flame remains at this binder

width, and further reduction of thickness leads to the approach to the deflagration limit (noted earlier) due to fuel starvation of the PVC flame. The overall postulated trend of burning rate is shown in Fig. 17. The present results are supportive of the postulated trend, but the available measurements demonstrate that trend only qualitatively in the mid-pressure range, and apparently do not encompass the relevant thickness range at low pressure. More extensive tests and improved methods may provide enough data to permit a more detailed interpretation (e.g., width of the fuel-rich region of the PVC vs pressure, etc).

AP-Filled Binder Laminae and Combustion Zone Microstructure

The tests on sandwiches with AP-filled binder laminae were largely exploratory, and detailed interpretation is probably premature. However, some general comments seem warranted and are made below primarily relative to the 6.9 MPa tests.

The results with 1:1 AP:binder ratio indicate that the fine AP particles did not establish their own individual AP, or AP-binder flames. This interpretation is based on the persistence of protrusion of, and smooth band on the adjoining AP, which in the present work have been interpreted as consequences of lateral heat drain from the thermal wave of the AP laminae into the endothermic binder. The increased width of the protruding region apparently reflects the higher thermal diffusivity of the fuel lamina with AP addition. Indeed, one might conclude that each AP particle vaporized endothermally just as a smooth band on the AP laminae is postulated to do, with the heat release being delayed until suitable conditions are reached in the larger mixing zone of the sandwich.

The same situation apparently prevailed also with the 7:3 AP:binder ratio when the lamina was thin. With a thicker lamina, the relatively smaller heat drain to the AP laminae from the gas phase flame part of the PVC region, and the larger volume of pre-mixed gas resulting from the AP in the binder allowed the flame to move in closer and enhance the overall burning rate. The persistence of smooth band and slight AP protrusion at the interface planes (Fig. 18) indicates that the flame still has not moved in near the filled binder lamina. The flame enhances the AP regression by heating a region of the AP surface somewhat removed from the interface (at the leading edge of the AP profile), while the heating closer to the interface is still not sufficient to compensate for the lateral heat drain to the fuel lamina. Presumably this situation would change with further increase in AP content in the fuel lamina. In a less fuel-rich lamina, the fuel dilution of the mixing fans from the individual oxidizer particles may be reduced enough for particles to acquire "their own" kinetically limited flamelets. Under those conditions, the main lamina flames may be less dominant, the heating of the interface AP by particle flames may permit normal AP deflagration and eliminate the protrusion at the interface. In effect, the filled lamina would burn at its own high rate, and pilot the burning of a truly "V"-shaped sample. However, it is important to note that this situation would correspond to a rather unusual propellant in which most of the AP was fine; high solids propellants would not normally have such high content of fine AP in the fuel volume.

Conclusion

The combined results have been interpreted in terms of a combustion zone

microstructure depicted in Fig. 13, which is applicable for thin-binder sandwiches burning at rocket motor pressures. The region of the flame near the burning surface (PVC region) involves a complex of interactive flames:

1. AP flame, including surface froth reactions and gas phase flame.
2. Kinetically limited pre-mixed flames between binder and AP vapors in the mixing fans.
3. Trailing diffusion-limited flames.

The heat flows in the solid and gas are decidedly two-dimensional on the scale of the relevant microstructure (Fig. 18). There tends to be a lateral heat drain in the solid, from the exothermic oxidizer to the endothermic fuel, with a resulting modification of the local oxidizer pyrolysis. The heat supply to the oxidizer surface is a maximum at some point, removed from the oxidizer-fuel interface plane, where there occurs a maximum excess of combined heat flow from the oxidizer-fuel flame and self-deflagration reactions over the heat drain through the solid to the fuel lamina. The dimensions of the regions involved are of the same order as the lateral dimensions of oxidizer particles in propellants, implying that the same non-one-dimensional considerations are important to propellants as well as sandwiches.

The results further indicate a singular transition in flame structure at low pressures or with small microstructural dimensions, associated with a concept called "stoichiometric tip withdrawal". In sandwich burning tests this led to a quench limit. A similar behavior in propellants is predicted to have conspicuous effect on dependence of burning rate on pressure, and on dependence of burning rate on oxidizer particle size.

The qualitative model provides a basis for design of future experiments and analyses concerning all aspects of combustion of AP-hydrocarbon binder propellants.

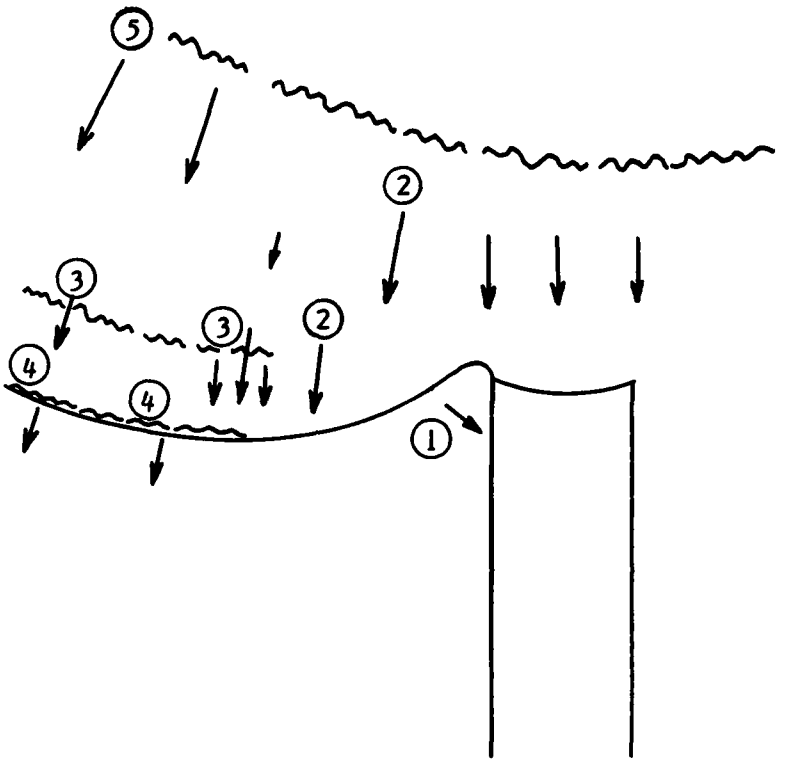

Fig. 18 Heat flow in the combustion zone of a sandwich.
1. Lateral heat flow into binder lamina.
2. Heat flow from AP-HC flame to smooth band.
3. Heat flow to AP surface from AP flame.
4. Heat flow from froth reaction into AP.
5. Lateral heat flow from AP-HC flame to AP outside of the PVC.

References

1. Powling, J., "Experiments Relating to the Combustion of Ammonium Perchlorate-Based Propellants," Proceedings of the 11th Symposium (International) on Combustion, 1966, The Combustion Institute, Pittsburgh, Pa., 1967, pp. 447-456.

2. Hightower, J. D. and Price, E. W., "Experimental Studies Relating to the Combustion Mechanism of Composite Propellants," Astronautica Acta, Vol. 14, 1968, pp. 11-21.

3. Hightower, J. D., Price, E. W., and Zurn, D. E., "Continuing Studies of the Combustion of Ammonium Perchlorate," CPIA Publication No. 162, Vol. I, December 1967, pp. 527-534.

4. Boggs, T. L. and Zurn, D. E., "The Deflagration of Ammonium Perchlorate-Polymeric Binder Sandwich Models," Combustion Science and Technology, Vol. 4, 1972, pp. 279-292.

5. Brown, W. E., Kennedy, J. R., and Netzer, D. W., "An Experimental Study of Ammonium Perchlorate-Binder Sandwich Combustion in Standard and High Acceleration Environments," Combustion Science and Technology, Vol. 6, 1972, pp. 211-222.

6. Abraham, M., III and Netzer, D. W., "Nonmetallized Solid Propellant Combustion in Standard and High Acceleration Environments," Combustion Science and Technology, Vol. 11, 1975, pp. 75-83.

7. Nadaud, L., "Models Used at ONERA To Interpret Combustion Phenomena in Heterogeneous Solid Propellants," Combustion and Flames, Vol. 12, 1968, pp. 177-195.

8. Ermolaev, B. S., Korotkov, A. I., and Frolov, Yu. V., "Laws of Combustion of a Solid Propellant Sandwich," Fizika Goreniya i Vzryva, Vol. 6, July-Sept. 1970, pp. 277-285.

9. Price, E. W., Handley, J. C., Panyam, R. R., Sigman, R. K. and Ghosh, A., "Combustion of Ammonium Perchlorate-Polymer Sandwiches," AIAA Journal, Vol. 19, March 1981, pp. 380-386.

10. Price, E. W., Sigman, R. D., and Panyam, R. R., "Combustion Mechanisms of Solid Propellants," Georgia Institute of Technology, Atlanta, Ga., September 1981.

11. Price, E. W., Panyam, R. R., and Sigman, R. K., "Microstructure of the Combustion Zone: Thin-Binder AP-Polymer Sandwiches," CPIA Publication No. 329, Vol. 1, Nov. 1980, pp. 37-51.

12. Hightower,J. D. and Price, E. W., "Combustion of Ammonium Perchlorate," Proceedings of the 11th Symposium (International) on Combustion, 1966, The Combustion Institute, Pittsburgh, Pa., 1967, pp. 463-472.

13. Boggs, T. L., Price, E. W., and Zurn, D. E., "The Deflagration of Pure and Isomorphously Doped Ammonium Perchlorate," Proceedings of the 13th Symposium (International) on Combustion, 1970, The Combustion Institute, Pittsburgh, Pa., 1971, pp. 995-1008.

14. Price, E. W., Handley, J. C., Strahle, W. C., Sheshadri, T. S., Sigman, R. K., and Ghosh, A., "Combustion Mechanisms of Solid Propellants," Georgia Institute of Technology, Atlanta, Ga., Sept. 1980.

15. Boggs, T. L., Zurn, D. E., Strahle, W. C., Handley, J. C., and Milkie, T. T., "Mechanisms of Combustion," Naval Weapons Center, NWC TP 5514, 1973.

16. Varney, A. M. and Strahle, W. C., "Experimental Combustion Studies of Two-Dimensional Ammonium Perchlorate-Binder Sandwiches," Combustion Science and Technology, Vol. 4, 1972, pp. 197-208.

17. Boggs, T. L., Zurn, D. E., and Netzer, D. W., "Ammonium Perchlorate Combustion: Effects of Sample Preparation; Ingredient Type; and Pressure, Temperature and Acceleration Environments," Combustion Science and Technology, Vol. 7, 1973, pp. 177-183.

18. Price, E. W. and Flandro, G. A., "Workshop Report: Combustion Zone Microstructure and Flow Effects," CPIA Publication No. 366, Vol. I, October 1982.

19. Cohen Nir, E., "An Experimental Study of the Low Pressure Limit for Steady Deflagration of Ammonium Perchlorate," Combustion and Flame, Vol. 20, 1973, pp. 419-435.

20. Guirao, C. and Williams, F. A., "A Model for Ammonium Perchlorate Deflagration between 20 and 100 atm," AIAA Journal, Vol. 9, July 1971, pp. 1345-1356.

21. Beckstead, M. W., Derr, R. L., and Price, C. F., "The Combustion of Solid Monopropellants and Composite Propellants," Proceedings of the 13th Symposium (International) on Combustion, 1970, The Combustion Institute, Pittsburgh, Pa., 1971, pp. 1047-1056.

22. Summerfield, M., Sutherland, G. S., Webb, M. J., Taback, H. V., and Hall, K. P., "Burning Mechanism of Ammonium Perchlorate Propellants," Solid Propellant Rocket Research, Progress in Astronautics and Rocketry Series, Vol. 1, Academic Press, New York, 1960, pp. 141-182.

23. Fenn, J. B., "A Phalanx Flame Model for the Combustion of Composite Solid Propellants," Combustion and Flame, Vol. 12, June 1968, pp. 201-216.

24. Belyaev, A. F. and Backman, N. N., "Theory of Burning of Powders and Solid Rocket Propellants (Review)," Combustion, Explosion and Shock Waves, Vol. 2, Winter 1966, pp. 1-17.

25. Beckstead, M. W., Derr, R. L., and Price, C. F., "A Model of Solid Propellant Combustion Based on Multiple Flames," AIAA Journal, Vol. 8, Dec. 1970, pp. pp. 2200-2206.

26. Hightower, J. D. and Price, E. W., "Two-Dimensional Experimental Studies of the Combustion Zone of Composite Propellants," CPIA Publication No. 105, Vol. 1, May 1966, pp. 421-435.

27. Strunin, V. A., D'yakov, V. A., and Manelis, G. B., "Influence and Disperseness of Components on Combustion Characteristics of a Mixed Composition," Fizika Goreniya i Vzryva, Vol. 17, Jan.-Feb. 1981, pp. 19-23.

28. Cohen, N. S., Fleming, R. W., and Derr, R. L., "Role of Binders in Solid Propellant Combustion," AIAA Journal, Vol. 12, No. 2, 1974, pp. 212-218.

29. Phillips, H., "Flame in a Buoyant Methane Layer," Proceedings of the Tenth Symposium (International) on Combustion, 1964, The Combustion Institute, Pittsburgh, Pa., 1965, pp. 1277-1283.

30. Schultz, R., Green, L., Jr., and Penner, S. S., "Studies of the Decomposition Mechanism, Erosive Burning, Sonance and Resonance for Solid Composite Propellants," Combustion and Propulsion, Proceedings of Third AGARD Colloquium, Pergamon Press, New York, 1958, pp. 367-420.

31. Bakhman, N. N. and Librovich, V. B., "Flame Propagation Along Solid Fuel-Solid Oxidizer Interface," Combustion and Flame, Vol. 15, Oct. 1970, pp. 143-155.

32. Povinelli, L. A., "Summary Report on the Nature of Ammonium Perchlorate Deflagration," CPIA Publication No. 192, Vol. 1, p. 372.

33. Williams, F. A., "Combustion Theory," The Fundamental Theory of Chemically Reacting Flow Systems," Addison-Wesley Publishing Company, Reading, Mass., p. 42.

34. Culick, F. E. C., "An Elementary Calculation of the Combustion of Solid Propellants," Astronautica Acta, Vol. 14, 1969, pp. 171-181.

DISTRIBUTION LIST

	No. Copies
Assistant Secretary of the Navy (R, E, and S) Room 5E 731 Pentagon Washington, DC 20350 Attn: Dr. L. V. Schmidt	1
Scientific Advisor Commandant of the Marine Corps Code RD-1 Washington, DC 20380 Attn: Dr. A. L. Slafkosky	1
Office of Naval Research Mechanics Division Code 432 Arlington, VA 22217 Attn: Dr. A. D. Wood	1
Office of Naval Research Mechanics Division Code 432 Arlington, VA 22217 Attn: Dr. Richard S. Miller	10
Office of Naval Research Code 260 Arlington, VA 22217 Attn: Mr. David Siegel	1
Office of Naval Research Western Office 1030 East Green Street Pasadena, CA 91106 Attn: Dr. R. J. Marcus	1
Office of Naval Research East Central Regional Office 666 Summer Street, Bldg. 114-D Boston, MA 02210 Attn: Dr. Larry Peebles	1
Office of Naval Research San Francisco Area Office One Hallidie Plaza, Suite 601 San Francisco, CA 94102 Attn: Dr. Phillip A. Miller	1
Aerojet Solid Propulsion Company P. O. Box 13400, Bldg. 2019/Dept. 4350 Sacramento, CA 95813 Attn: Mr. Michael J. Ditore	1

	No. Copies
Aerojet Strategic Propulsion Co. P. O. Box 15699C Sacramento, CA 95813 Attn: Dr. R. L. Lou	1
Aerospace Corporation P. O. Box 92957 Los Angeles, CA 90045 Attn: Ellis M. Landsbaum	1
U. S. Air Force Academy FJSRL/NC USAF Academy, CO 80840 Attn: Dr. John S. Wilkes, Jr.	1
AFATL Code DLDL Eglin AFB, FL 32542 Attn: Mr. Otto K. Heiney	1
Air Force Office of Scientific Research Directorate of Aerospace Sciences Bolling Air Force Base Washington, DC 20332 Attn: Dr. L. H. Caveny	1
Air Force Office of Scientific Research Directorate of Chemical Sciences Bolling Air Force Base Washington, DC 20332 Attn: Mr. Donald L. Ball	1
AFRPL Code PACC Edwards AFB, CA 93523 Attn: Mr. Wayne Roe	1
AFRPL Code MKP/MS24 Edwards AFB, CA 93523 Attn: Mr. R. Geisler	1
AFRPL Code DYSC Edwards AFB, CA 93523 Attn: Mr. Daweel George	1

	No. Copies
AFRPL Code LK Edwards AFB, CA 93523 Attn: LTC B. Loving	1
AFRPL Code MKPA Edwards AFB, CA 93523 Attn: Dr. F. Roberto	1
AFRPL Code CA Edwards AFB, CA 93523 Attn: Dr. R. R. Weiss	1
Anal-Syn Lab Inc. P. O. Box 547 Paoli, PA 19301 Attn: Dr. V. J. Keenan	1
Army Ballistic Research Labs ARRADCOM Code DRDAR-BLI Aberdeen Proving Ground, MD 21005 Attn: Mr. J. M. Frankle Dr. Ingo W. May Mr. L. A. Watermeier	3
Army Ballistic Research Labs ARRADCOM Code DRDAR-BLP Aberdeen Proving Ground, MD 21005 Attn: Dr. A. W. Barrows	1
Army Ballistic Research Labs ARRADCOM Code DRDAR-BLT Aberdeen Proving Ground, MD 21005 Attn: Dr. Philip Howe	1
Army Frankford Arsenal Bridge & Tacony Streets Philadelphia, PA 19137 Attn: J. Lannon	1
HQ US Army Material Development Readiness Command Code DRCDE-DW 5011 Eisenhower Avenue Room 8N42 Alexandria, VA 22333 Attn: Mr. S. R. Matos	1

	No. Copies
Army Missile Command Code DRSMI-R Redstone Arsenal, AL 35898 Attn: Dr. R. G. Rhoades	1
Army Missile Command Code DRSMI-RKL Redstone Arsenal, AL 35898 Attn: Dr. W. W. Wharton	1
Army Research & Development Command ARRADCOM Code LCWSL Dover, NJ 07802	1
Army Research & Development Command ARRADCOM Code DRDAR-SCA-PE Dover, NJ 07802 Attn: Mr. L. Stiefel	1
Army Research & Development Command ARRADCOM Code DRDAR-LCE Dover, NJ 07802 Attn: Dr. R. F. Walker	1
U. S. Army Research Office Chemical & Biological Sciences Div. P. O. Box 12211 Research Triangle Park, NC 27709	1
Atlantic Research Corp. 4390 Cherokee Ave. Alexandria, VA 22314 Attn: Dr. C. B. Henderson Dr. Merill K. King	2
Atlantic Research Corp Pine Ridge Plant 7511 Wellington Rd. Gainesville, VA 22065 Attn: Mr. R. H. W. Waesche	1
Brigham Young University Provo, UT 84601 Attn: Dr. Merrill W. Beckstead	1

DISTRIBUTION LIST

	No. Copies
British Embassy Munitions Directorate Propellants and Explosives Defence Equipment Staff 3100 Massachusetts Ave. Washington, DC 20008 Attn: Dr. T. Sinden	1
California Institute of Tech. Graduate Aeronautical Lab Pasadena, CA 91125 Attn: Prof. W. G. Knauss	1
California Institute of Tech. Dept. of Chemical Engineering Pasadena, CA 91125 Attn: Prof. N. W. Tschoegl	1
California Institute of Tech. 204 Karman Lab 1201 E. California St. Pasadena, CA 91109 Attn: Fred E. C. Culick	1
California Institute of Tech. Jet Propulsion Laboratory 4800 Oak Grove Drive Pasadena, CA 91103 Attn: Leon D. Strand	1
Calspan Corporation P. O. Box 235 Buffalo, NY 14221 Attn: Edward B. Fisher	1
Catholic Univ. of America Physics Department 520 Michigan Ave., NE Washington, DC 20017 Attn: Prof. T. Litovitz	1
Mr. Norman Cohen 858-A Pine Ave. Redlands, CA 92373	1
Cornell University School of Chemical Engineering Olin Hall Ithaca, NY 14853 Attn: Prof. F. Rodriguez	1
Defense Technical Information Center Code DTIC-DDA-2 Cameron Station Alexandria, VA 22314	12
Georgia Institute of Tech. School of Aerospace Engineering Atlanta, GA 30332 Attn: Prof. Edward Price	1
Hercules Inc. Aerospace Division Alleghany Ballistic Lab P. O. Box 210 Washington, DC 21502 Attn: Dr. Rocco C. Musso Dr. R. R. Miller	2
Hercules Inc. Bacchus Works P. O. Box 98 Magna, UT 84044 Attn: Dr. E. H. Debutts Dr. James H. Thacher Dr. K. McCarty	3
Hercules Inc. Eglin Code AFATL/DLDL Eglin AFB, FL 32542 Attn: Dr. Ronald L. Simmons	1
Hercules Inc. Aerospace Division P. O. Box 210 Cumberland, MD 21502 Attn: Dr. Kenneth O. Hartman	1
Hercules, Inc. P. O. Box 548 McGregor, TX 76657 Attn: Mr. William G. Haymes	1
IBM Research Lab D42.282 San Jose, CA 95193 Attn: Dr. Thor L. Smith	1
Institute for Defense Analyses 400 Army-Navy Drive Arlington, VA 22202 Attn: R. C. Oliver	1
Johns Hopkins University APL Chemical Propulsion Info. Agency Johns Hopkins Road Laurel, MD 20810 Attn: Mr. Thomas W. Christian Mr. Theodore M. Gilliland	2
Lawrence Livermore Laboratory University of California Code L-324 Livermore, CA 94550 Attn: Dr. R. McGuire	1
Lockheed Missile & Space Co. Code 83-10, Bldg. 154 P. O. Box 504 Sunnyvale, CA 94088 Attn: Dr. Jack Linsk	1
Lockheed Missile & Space Co. Dept. 52-35, Bldg. 204/2 3251 Hanover Street Palo Alto, CA 94304 Attn: Dr. H. P. Marshall	1
Los Alamos Scientific Lab Code NSP/DOD, MS-245 P. O. Box 1663 Los Alamos, NM 87545 Attn: Dr. B. C. Craig	1
Los Alamos Scientific Lab Mail Stop 920 Los Alamos, NM 87545 Attn: Ms. Joan L. Janney	1
Los Alamos Scientific Lab Code WX-2, MS-952 P. O. Box 1663 Los Alamos, NM 87545 Attn: Dr. R. L. Rabie	1
Los Alamos Scientific Lab Code WX-2 P. O. Box 1663 Los Alamos, NM 87545 Attn: Dr. R. Rogers	1
Los Alamos Scientific Lab P. O. Box 1663 Los Alamos, NM 87545 Attn: Dr. J. M. Walsh	1
NASA/George C. Marshall Space Flight Center Code EP 25 Huntsville, AL 35812 Attn: J. Q. Miller	1
NASA/George C. Marshall Space Flight Center Code EP 24 Huntsville, AL 35812 Attn: Robert J. Richmond	1
NASA/HQ Code RP 600 Independence Ave., SW, Rm. 625 Washington, DC 20546 Attn: Frank W. Stephenson, Jr.	1
Naval Air Systems Command Code 330 Washington, DC 20361 Attn: Mr. R. Brown	1
Naval Air Systems Command Code AIR-310C Washington, DC 20360 Attn: Dr. H. Rosenwasser	1
Naval Air Systems Command Code 03P25 Washington, DC 20360 Attn: Mr. B. Sobers	1
Naval Air Systems Command Code NAIR-954-Tech Library Washington, DC 20361	1
Naval Explosives Dev. Engineering Department Assistant Director Naval Weapons Station Yorktown, VA 23691 Attn: Dr. L. R. Rothstein	1

DISTRIBUTION LIST

	No. Copies
Naval Explosive Ordnance Disposal Tech Center Code D Indian Head, MD 20640 Attn: Dr. Lionel Dickinson	1
Naval Materiel Command Strategic Systems Project Office Department of the Navy Room 901 Washington, DC 20376 Attn: Dr. J. F. Kincaid	1
Naval Materiel Command Strategic Systems Project Office Propulsion Unit Code SP 2731 Department of the Navy Washington, DC 20376	1
Naval Materiel Command Strategic Systems Project Office Department of the Navy Room 1048 Washington, DC 20376 Attn: Mr. E. L. Throckmorton	1
Naval Ocean Systems Center San Diego, CA 92152 Attn: Mr. Joe McCartney	1
Naval Ocean Systems Center Marine Sciences Division San Diego, CA 91232 Attn: Dr. S. Yamamoto	1
Naval Ordnance Station PM4 Indian Head, MD 20640 Attn: Mr. C. L. Adams	1
Naval Ordnance Station Code 5253 Indian Head, MD 20640 Attn: Mr. S. Mitchell	1
Naval Ordnance Station Indian Head, MD 20640 Attn: Mr. Peter L. Stang	1

	No. Copies
Naval Ordnance Station Code 525 Indian Head, MD 20640 Attn: Mr. C. M. Christensen	1
Naval Postgraduate School Dean of Research Monterey, CA 93940 Attn: Dr. William Tolles	1
Naval Postgraduate School Physics & Chemistry Dept. Monterey, CA 93940 Attn: Prof. Richard A. Reinhardt	1
Naval Postgraduate School Department of Aeronautics Monterey, CA 93940 Attn: Mr. David W. Netzer	1
Office of Naval Research Mechanics Division Code 432 Arlington, VA 22217 Attn: Dr. N. L. Basdekas	1
Naval Research Lab. Code 6100 Washington, DC 20375	1
Naval Research Lab. Code 6510 Washington, DC 20375 Attn: Dr. J. Schnur Dr. Elaine Oran	2
Naval Sea Systems Command Code SEA 64E Washington, DC 20362 Attn: Mr. R. Beauregard	1
Naval Sea Systems Command Code 62R3 Washington, DC 20362 Attn: Mr. G. Edwards	1
Naval Sea Systems Command NAV SEA 62R22 Crystal Plaza, Bldg. 6, Rm 806 Washington, DC 20362 Attn: Mr. Robert F. Cassel	1

	No. Copies
Naval Sea Systems Command Code 62R2 Washington, DC 20362 Attn: Mr. J. Murrin	1
Naval Ship Engineering Center Materials Branch Philadelphia, PA 19112 Attn: Mr. John Boyle	1
Naval Ship Research & Development Center Applied Chemistry Division Annapolis, MD 21401 Attn: Dr. G. Bosmajian	1
Naval Surface Weapons Center Commander Silver Spring, MD 20910 Attn: Mr. G. B. Wilmot	4
Naval Surface Weapons Center Code R04 White Oak Laboratory Silver Spring, MD 20910 Attn: Dr. D. J. Pastine	1
Naval Surface Weapons Center Code R10 White Oak Laboratory Silver Spring, MD 20910 Attn: Dr. S. J. Jacobs	1
Naval Surface Weapons Center Code R11 White Oak Laboratory Silver Spring, MD 20910 Attn: Dr. H. G. Adolph Dr. T. Hall Dr. M. J. Kamlet Dr. K. F. Mueller	4
Naval Surface Weapons Center Code R13 White Oak Laboratory Silver Spring, MD 20910 Attn: Dr. E. Zimmet Dr. R. Bernecker	2

	No. Copies
Naval Surface Weapons Center Code R16 Indian Head, MD 20640 Attn: Dr. T. D. Austin	1
Naval Surface Weapons Center Code R101 Indian Head, MD 20640 Attn: Mr. G. L. Mackenzie	1
Naval Surface Weapons Center Code R121 White Oak Laboratory Silver Spring, MD 20910 Attn: Mr. M. Stosz	1
Naval Surface Weapons Center Code R122 White Oak Laboratory Silver Spring, MD 20910 Attn: Mr. L. Roslund	1
Office of Naval Technology Chief MAT Code 0716 Washington, DC 20360 Attn: Dr. A. Faulstich	1
Office of Naval Technology Chief of Naval Material MAT Code 0712 Washington, DC 20360 Attn: LCDR J. Walker	1
Naval Underwater Systems Center Energy Conversion Dept. Code 5B331 Newport, RI 02840 Attn: Mr. Robert S. Lazar	1
Naval Weapons Center Code 385 China Lake, CA 93555 Attn: Dr. A. Amster Dr. A. Nielsen	2
Naval Weapons Center Code 388 China Lake, CA 93555 Attn: Mr. T. L. Boggs Dr. R. L. Derr Dr. R. Reed, Jr.	3

DISTRIBUTION LIST

	No. Copies
Naval Weapons Center Code 3205 China Lake, CA 93555 Attn: Mr. Lee N. Gilbert Dr. L. Smith Dr. C. Thelen	3
Naval Weapons Center Code 3272 China Lake, CA 93555 Attn: Mr. R. McCarten	1
Naval Weapons Center Code 3858 China Lake, CA 93555 Attn: Dr. E. Martin	1
Naval Weapons Support Center Code 5042 Crane, IN 47522 Attn: Dr. B. Douda	1
Northwestern University Dept. of Civil Engineering Evanston, IL 60201 Attn: Prof. J. D. Achenbach	1
Pennsylvania State University Dept. of Mechanical Engineering University Park, PA 16802 Attn: Prof. Kenneth Kuo	1
Princeton Combustion Research Laboratories, Inc. 1041 U. S. Highway One North Princeton, NJ 08540 Attn: Dr. Martin Summerfield	1
Princeton University School of Engineering and Applied Sciences Dept. of Mech. Eng. & Aero. Eng. The Engineering Quadrangle Princeton, NJ 08544 Attn: Dr. Forman A. Williams	1
Purdue University School of Mechanical Engineering TSPC Chaffee Hall West Lafayette, IN 47906 Attn: Mr. John R. Osborn	1
Rockwell International Corp. Rocketdyne Division BA08 6633 Canoga Ave. Canoga Park, CA 91304 Attn: Mr. Joseph E. Flanagan	1
Rohm and Haas Company Huntsville, AL 35801 Attn: Dr. H. Shuey	1
Sandia Laboratories Division 2513 P. O. Box 5800 Albuquerque, NM 87185 Attn: Dr. S. Sheffield	1
Science Applications, Inc. Suite 423 20335 Ventura Blvd. Woodland Hills, CA 91364 Attn: Mr. R. B. Edelman	1
Space Sciences, Inc. 135 Maple Avenue Monrovia, CA 91016 Attn: Dr. M. Farber	1
Southwest Research Institute Institute Scientist P. O. Drawer 28510 San Antonio, TX 78228 Attn: Mr. William H. McLain	1
SRI International 333 Ravenswood Ave. Menlo Park, CA 94025 Attn: Mr. M. Hill Dr. Y. M. Gupta	2
Texas A & M University Dept. of Civil Engineering College Station, TX 77843 Attn: Prof. Richard A. Schapery	1
Thiokol Corporation Elkton Division P. O. Box 241 Elkton, MD 21921 Attn: Mr. E. S. Sutton Dr. C. W. Vriesen	2
Thiokol Corporation Government Systems Group Technical Director P. O. Box 9258 Ogden, Utah 84409 Attn: Dr. T. F. Davidson	1
Thiokol Corporation Huntsville Division Huntsville, AL 35807 Attn: Dr. D. A. Flanigan Mr. G. F. Mangum Mr. J. D. Byrd	3
Thiokol Corporation Wasatch Division P. O. Box 524 Brigham City, UT 84302 Attn: Dr. J. C. Hinshaw Mr. John A. Peterson Dr. G. Thompson	3
United Technologies Corp. Chemical Systems Division P. O. Box 358 Sunnyvale, CA 94088 Attn: Dr. Robert S. Brown Dr. C. M. Frey	2
University of Akron Institute of Polymer Science Akron, OH 44325 Attn: Prof. Alan N. Gent	1
University of California Berkeley, CA 94720 Attn: Prof. A. G. Evans	1
University of California Dept. of Chemistry 405 Hilgard Ave. Los Angeles, CA 90024 Attn: Prof. M. D. Nicol	1
University of Delaware Department of Chemistry Newark, DE 19711 Attn: Dr. T. C. Brill	1
University of Illinois AE Dept. Transportation Building, Room 105 Urbana, IL 61801 Attn: Dr. Herman Krier	1
University of Maryland Dept. of Mechanical Engineering College Park, MD 20742 Attn: Prof. R. W. Armstrong	1
University of Southern California Mechanical Engineering Dept. OHE 200 Los Angeles, CA 90007 Attn. Dr. M. Gerstein	1
University of Utah Salt Lake City, UT 84112 Attn: Dr. G. A. Flandro	1
University of Utah Dept. of Mech. & Ind. Eng. MEB 3008 Salt Lake City, UT 84112 Attn: Dr. Stephen Swanson	1
University of Waterloo Dept. of Mechanical Engineering Waterloo, Ontario CANADA Attn: Dr. Clarke E. Hermance	1
Washington State University Dept. of Physics Pullman, WA 99163 Attn: Prof. G. D. Duvall Prof. T. Dickinson	2
Whittaker Corporation Bermite Division 22116 W. Soledad Canyon Road Saugus, CA 90024 Attn: Mr. L. Bloom	1